A Raman spectroscopic study of the different vanadate-groups in solid-state compounds, model case - mineral phases vésigniéite, $BaCu_3(VO_4)_2(OH)_2$, and volborthite, $Cu_3V_2O_7(OH)_2 \cdot 2H_2O$

Ray L. Frost, [1] • Sara J. Palmer, [1] Jiří Čejka, [1,2] Jiří Sejkora, [2] Jakub Plášil, [2] Silmarilly Bahfenne [1] and Eloise C. Keeffe [1]

[1] Chemistry Discipline, Faculty of Science and Technology, Queensland University of Technology, GPO Box 2434, Brisbane Queensland 4001, Australia.

[2] National Museum, Václavské náměstí 68, CZ-115 79 Praha 1, Czech Republic.

Abstract

Raman spectroscopy has been used to study vanadates in the solid state. The molecular structures of the vanadate minerals vésigniéite, $BaCu_3(VO_4)_2(OH)_2$, and volborthite, $Cu_3V_2O_7(OH)_2.2H_2O$, have been studied by Raman spectroscopy and infrared spectroscopy. The spectra are related to the structure of the two minerals. The Raman spectrum of vésigniéite is characterized by two intense bands at 821 and 856 cm^{-1} assigned to $\nu_1 (VO_4)^{3-}$ symmetric stretching modes. A series of infrared bands at 755, 787 and 899 cm^{-1} are assigned to the $\nu_3 (VO_4)^{3-}$ antisymmetric stretching vibration mode. Raman bands at 307 and 332 cm^{-1} and at 466 and 511 cm^{-1} are assigned to the ν_2 and $\nu_4 (VO_4)^{3-}$ bending modes. The Raman spectrum of volborthite is characterized by the strong band at 888 cm^{-1}, assigned to the ν_1 (VO_3) symmetric stretching vibrations. Raman bands at 858 and 749 cm^{-1} are assigned to the ν_3 (VO_3) antisymmetric stretching vibrations, those at 814 cm^{-1} to the ν_3 (VOV) antisymmetric vibrations, that at 508 cm^{-1} to the ν_1 (VOV) symmetric stretching vibration, and bands at 442 and 476 cm^{-1} and 347 and 308 cm^{-1} to the ν_4 (VO_3) and ν_2 (VO_3) bending vibrations, respectively. The spectra of vésigniéite and volborthite are similar especially in the region of skeletal vibrations, albeit their crystal structures differ.

KEYWORDS: solid state vanadates, vésigniéite, volborthite, hydroxyl, Raman spectroscopy

• Author to whom correspondence should be addressed (r.frost@qut.edu.au)

INTRODUCTION

The monoclinic mineral vésigniéite, $BaCu_3(VO_4)_2(OH)_2$, forms lamellar pseudohexagonal crystals and platy aggregates [1] . The mineral is found in many occurrences worldwide, including uranium-vanadium deposits and oxide zones of ore deposits. The crystal structure of vésigniéite with space group *C*2/*m*, is principally composed of CuO_6 polyhedra linked in layers with the barium atoms in between the layers. The edge-sharing CuO_6 tetragonal bipyramids form chains parallel to the [010] and [110] axes. The chains are interlocked to form layers parallel to [001]. Each of the VO_4 tetrahedra is linked to three CuO_6 and one BaO_{12} polyhedra [2-4] (Fig. 1). The mineral volborthite, $Cu_3(V_2O_7)(OH)_2.2H_2O$, is monoclinic, pseudohexagonal and forms typical rosette like aggregates of scaly crystals [1]. Volborthite is an uncommon secondary mineral formed in the oxidized zone of vanadium-bearing hydrothermal mineral deposits [1]. The crystal structure of volborthite and its synthetic analogue has been studied (see [5-7]). The basic structure of monoclinic volborthite is a sheet-like structure with copper oxide/hydroxide layers that are held together by the pyrovanadate O_3V-O-VO_3 groups (Fig. 2). These layers are stacked within layers of water. The crystal structure of the new mineral species martyite, $Zn_3(V_2O_7)(OH)_2.2H_2O$, is isostructural to that of volborthite [8]. Synthetic vésigniéite and volborthite have been studied in order to derive information about the intrinsic properties of the spin-1/2 kagome antiferromagnet [9, 10].

Few published data exist on the Raman spectra for minerals which contain $(VO_4)^{3-}$ [11]. There are approximately 70 minerals which contain $(VO_4)^{3-}$ groups [1]. In basic pH conditions these form simple structures with VO_4 tetrahedra but with increasing acidity these tetrahedra link into chains and then into polynuclear groups of square dipyramids or distorted octahedra [12]. Interest in the minerals arises from their ferroelectric properties [9,10]. As part of a comprehensive study of the large group of supergene minerals [24-26] and especially the molecular structure of minerals containing oxyanions using IR and Raman spectroscopy, we report the Raman spectra of vésigniéite and volborthite and relate the spectra to the molecular structure and the crystal chemistry of these vanadate type mineral.

EXPERIMENTAL

Minerals

The studied sample of volborthite originated from the historical occurrence at Middle Ural (Permskaya Oblast), Russia; the sample of vésigniéite was found at mine dumps of the Vrančice deposit, central Bohemia, Czech Republic. These samples are deposited in the mineralogical collections of the National Museum Prague. They were analysed for phase purity by X-ray powder diffraction and no minor significant impurities were found. Polished sections of both samples were analysed by Cameca SX100 microprobe system in wavelength dispersion mode for chemical composition, the water contents were calculated on the basis of charge balance and theoretical content of $2H_2O$ in volborthite.

The refined unit-cell parameters of studied volborthite for monoclinic space group *C*2/*m*, *a* = 10.564(9), *b* = 5.877(4), *c* = 7.204(2) Å, β = 94.82(4)° and *V* = 445.7(3) Å^3, are comparable with the data published for this mineral phase [5]. The results of chemical analyses (Table 1) lead to empirical formula $Cu_{3.00}(V_{1.97}Si_{0.03})_{\Sigma 2.00}O_7(OH)_{1.96} \cdot 2H_2O$ on the basis of (V+Si) = 2 *apfu (atoms per formula unit)*. The presence of pyrovanadate (V_2O_7) groups in the crystal structure shows that no phosphate or arsenates in vanadates (the usual isomorphism) was observed.

The refined unit-cell parameters of studied vésigniéite for monoclinic space group *C*2/*m*, *a* = 10.251(2), *b* = 5.920(1), *c* = 7.71(2) Å, β = 116.27(1)° and *V* = 420.0(2) Å^3, agree very well with the data published for this mineral phase [4]. The results of chemical analyses (Table 1) lead to empirical formula $(Ba_{0.87}Al_{0.06}K_{0.03}Ca_{0.02}Fe_{0.01})_{\Sigma 0.99}(Cu_{3.02}Zn_{0.01})_{\Sigma 3.03}$ $[(VO_4)_{1.78}(SiO_4)_{0.11}(AsO_4)_{0.08}(PO_4)_{0.03}]_{\Sigma 2.00}(OH)_{1.98}$ on the basis of (V+Si) = 2 *apfu*.

Raman spectroscopy

Crystals of vésigniéite and volborthite were placed on a polished metal surface on the stage of an Olympus BHSM microscope, which is equipped with 10x, 20x, and 50x objectives. The microscope is part of a Renishaw 1000 Raman microscope system, which also includes a monochromator, a filter system and a CCD detector (1024 pixels). The Raman spectra were excited by a Spectra-Physics model 127 He-Ne laser producing highly polarised light at 633 nm and collected at a nominal resolution of 2 cm^{-1} and a precision of ± 1 cm^{-1} in the range between 200 and 4000 cm^{-1}. Repeated acquisition on the crystals using the highest

magnification (50x) were accumulated to improve the signal to noise ratio in the spectra. Spectra were calibrated using the 520.5 cm^{-1} line of a silicon wafer. Alignment of all crystals in a similar orientation has been attempted and achieved. However, differences in intensity may be observed due to minor differences in the crystal orientation.

Infrared spectroscopy

Infrared spectra of both mineral samples were recorded by micro diffuse reflectance method (DRIFTS) on a Nicolet Magna 760 FTIR spectrometer (range 4000-600 cm^{-1}, resolution 4 cm^{-1}, 128 scans, 2 level zero filling, Happ-Genzel apodization), equipped with Spectra Tech InspectIR micro FTIR accessory. Each sample of amount less than 0.050 mg was mixed without using pressure with KBr. Samples were immediately recorded together with the same KBr as a reference.

Spectral manipulation such as baseline correction/adjustment and smoothing were performed using the Spectracalc software package GRAMS (Galactic Industries Corporation, NH, USA). Band component analysis was undertaken using the Jandel 'Peakfit' software package that enabled the type of fitting function to be selected and allows specific parameters to be fixed or varied accordingly. Band fitting was done using a Lorentzian-Gaussian cross-product function with the minimum number of component bands used for the fitting process. The Lorentzian-Gaussian ratio was maintained at values greater than 0.7 and fitting was undertaken until reproducible results were obtained with squared correlations of r^2 greater than 0.995.

RESULTS and DISCUSSION

Factor Group Analysis

The primitive unit cell of vésigniéite and volborthite contains one formula unit and thus 18 and 22 atoms respectively. In vésigniéite, the two inequivalent Cu atoms and Ba atom occupy C_2 sites whereas V, O_1, O_2, O_3, O_4, and H_1 atoms occupy C_s sites. Each atom on C_2 sites gives vibrations of A and $2B$ symmetry, which split under C_{2h} crystal symmetry to A_g, A_u, $2B_g$ and $2B_u$, whereas each atom on C_s sites gives vibrations of $2A'$ and A'', splitting to

133 $2A_g$, $2B_u$, B_g and A_u. A total of 51 allowable modes were given. The symmetry of VO_4 is
134 reduced from the ideal tetrahedral symmetry (T_d) to C_s. Under T_d symmetry there are A_1, E,
135 and $2F_2$ modes. On a C_s site the A_1 mode translates to A', E splits to A' and A", and F_2 to $2A$'
136 and A". Correlating this to a C_{2h} crystal system, each A' mode splits to A_g and B_g, and each
137 A" to B_g and A_u. The splitting pattern is summarised in the table below. All modes are
138 active. There are 18 internal modes associated with the VO_4 ion. The symmetric stretch (A_1)
139 gives rise to only A_g in the Raman spectrum, and B_u in infrared, and the antisymmetric stretch
140 (F_2) gives rise to $2A_g$ and $1B_g$ in the Raman spectrum, and $2B_u$ and A_u in infrared.

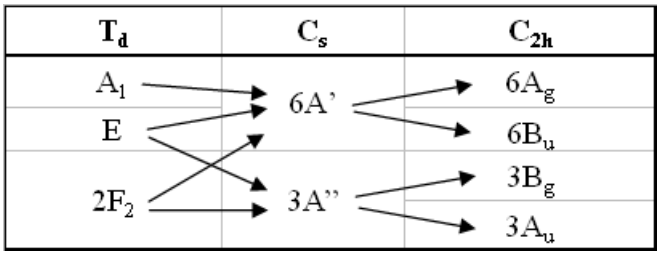

141

142

143 In volborthite, the two inequivalent Cu atoms and O_1 atom occupy C_{2h} sites, whereas V, O_2,
144 O_3, O_4, and O_w atoms occupy C_s sites and two H atoms on C_1 sites. Each atom on C_{2h} gives
145 A_g, B_u, B_g and A_u modes, those on C_1 sites each give $3A$ modes which split to $3A_g$, $3B_u$, $3B_g$
146 and $3A_u$, and those on C_s sites split as above. A total of 63 modes were given. Rationalising
147 the vibrations of the O_3V-O-VO_3 unit, our analysis starts on a VO_3 group with C_{3v} symmetry.
148 The vibrations of a C_{3v} molecule ($2A_1$ and $2E$) are correlated to the D_{3d} symmetry of an
149 isolated V_2O_7 anion and then to the C_{2h} crystal symmetry. The splitting pattern is
150 summarised in the following table. The symmetric stretch of the V-O-V bond gives rise to
151 $2A_g$ modes, and the antisymmetric stretch will only appear in the infrared spectrum as $2B_u$
152 bands. Degenerate stretching vibrations give rise to $2A_g$ and $2B_g$ modes in the Raman
153 spectrum and $2A_u$ and $2B_u$ modes in the infrared.

C_{3v}	D_{3d}	C_{2h}
$2A_1$	$2A_{1g}$	$2A_g$
	$2A_{2u}$	$2B_u$
2E	$2E_g$	$2A_g$, $2B_g$
	$2E_u$	$2A_u$, $2B_u$

Background on the spectroscopy of vanadates

According to data in the references [14, 16, 17, 19-21, 27, 28], free vanadate unit $(VO_4)^{3-}$, possessing the T_d symmetry, is characterized by four vibrations: the ν_1 (A_1) symmetric stretching mode (Raman active, 878 cm^{-1}), the ν_2 (E) doubly degenerate symmetric bending mode (Raman active, 345 cm^{-1}), the ν_3 (F_2) triply degenerate antisymmetric stretching mode (Raman and infrared active, 825 cm^{-1}), and the ν_4 (F_2) triply degenerate antisymmetric bending mode (Raman and infrared active, 480 cm^{-1}). Through symmetry lowering the degeneracy is removed and all modes become both Raman and infrared active. The fundamental stretching modes can also give rise to combination and overtones, which are generally detectable by Raman and/or infrared spectroscopy. Such modes can be infrared active and give rise to a broad complex absorption in the region 1900 to 1600 cm^{-1} [21]. According to Griffith [16], three skeletal vibrations are expected in the spectra of $(V_2O_7)^{4-}$ units, the $\nu_{V\text{-}O\text{-}V}$ antisymmetric stretching vibration, the $\nu_{V\text{-}O\text{-}V}$ symmetric stretching vibration, and the $\delta_{V\text{-}O\text{-}V}$ bending vibration [16]. The $(V_2O_7)^{4-}$ units also show bands arising from the symmetric and antisymmetric stretching vibrations of the (VO_3) units and a (VO_3) bending mode [16]. Thus, this may be characterized as follows: the ν_1 (VO_3) symmetric stretching mode at 877 cm^{-1}, the ν_3 (VO_3) antisymmetric stretching mode at 850 cm^{-1}, the ν_3 (V-O-V) antisymmetric stretching mode at 810 cm^{-1}, the ν_1 (V-O-V) symmetric stretching mode at 503 cm^{-1}, and the δ (V-O-V) bending mode at 228 cm^{-1}. As mentioned above, symmetry lowering can be connected with the Raman and infrared activation of all vibrations and the splitting of the degenerate vibrations. From the comparison of predicted and expected Raman and infrared bands related to the $(VO_4)^{3-}$ and $(V_2O_7)^{4-}$ vibrations, it is inferred that the skeletal vibrations of both units may overlap.

Levitt and Condrate based upon the analysis of the spectra of lead apatites (part of the pyromorphite group minerals) reported the ν_2 band for vanadinites at 320 cm^{-1} [13]. Ross reported the infrared and Raman spectra of the free VO_4^{3-} ion [14]. The ν_1 band was observed at 874 cm^{-1}; ν_2 at 345 cm^{-1}; ν_3 at 855 cm^{-1} and ν_4 at 345 cm^{-1}. Ross [14] also reported the ν_3 modes of vanadinites at 800 and 736 cm^{-1} and the ν_4 modes around 419, 380 and 322 cm^{-1}. In this work the position of the ν_1 and ν_2 vibrations were not tabled. Gadsen also reported the infrared spectrum of vanadinites [15]. The ν_3 mode is reported as occurring between 700 and 900 cm^{-1} and the ν_4 mode between 300 and 410 cm^{-1}. The ν_1 mode, which is not observed in the infrared spectrum (as the vibration is inactive), was suggested to be at around 870 cm^{-1}. Griffith described the Raman spectra of vanadates in solution [16] and the Raman spectra of vanadinites [17]. Single crystal Raman spectra of a vanadinite at 298K have been reported [18]. Some vanadates, the same as other tetrahedral anions such as sulphates, have their symmetry reduced through acting as monodentate and bidentate ligands [19]. In the case of bidentate behaviour both bridging and chelating ligands are known. This reduction in symmetry is observed by the splitting of the ν_3 and ν_4 in infrared spectra into two components under C_{3v} symmetry and into 3 components under C_{2v} symmetry. Early investigations of the vibrational spectra of apatites of lead including vanadinite were limited to mid-IR studies. Some relations concerning the Raman and infrared spectra of various vanadate units may be inferred from the paper by Ribeiro-Claro *et al.* [20] and Busca [21]. The Raman and infrared spectra of vésigniéite have been published and interpreted by Botto and Deliens [2] without any knowledge of the detailed crystal structure of vésigniéite. The Raman spectra of three volborthite samples were published in the RRUFF's database without giving any information on wavenumbers of observed bands (http://rruff.info/volborthite/names/asc/R050216,R050249,R070710). Crystal chemical aspects of vanadium including polyhedral geometries, characteristic bond valences and polymerization of VO_a polyhedra and a crystal-chemical approach to the composition and occurrence of vanadium minerals were discussed by Schindler *et al.* [22, 23].

Raman and infrared spectra of vésigniéite

The Raman and infrared spectra of vésigniéite and volborthite over the full wavenumber range are displayed in Figs. 3 and 4 respectively. These figures show the

relative intensities of the bands in the spectra of the two minerals. The figures show the marked similarity of the spectra of the two minerals.

Botto and Deliens [2] reported the Raman and infrared spectroscopic and thermal analysis of the vésigniéite mineral and also elucidated the factor group analysis of the mineral structure. The Raman spectrum of vésigniéite in the 600 to 1200 cm^{-1} region is displayed in Fig. 5. Raman bands are observed at 750, 821 and 856 cm^{-1} with a broad low intensity band at 1050 cm^{-1}. The bands at 821 and 856 cm^{-1} are assigned to the ν_1 $(VO_4)^{3-}$ symmetric stretching vibration. In aqueous solution the symmetric stretching band is found at 824 cm^{-1}. The observation of two bands as symmetric stretching modes provides evidence for the non-equivalence of vanadate anions in the vésigniéite structure. X-ray diffraction only detects an average of the mineral structure and thus only shows all vanadates units as equivalent. Raman spectroscopy detects structure at a molecular level as opposed to a lattice unit. However, only one symmetrically distinct $(VO_4)^{3-}$ unit was inferred from the X-ray crystal structure analysis of vésigniéite [4]. The low intensity band at 750 cm^{-1} is attributed to the ν_3 $(VO_4)^{3-}$ antisymmetric stretching vibration. Botto and Deliens [2] proposed the reduction of the symmetry of the vanadate anion in the vésigniéite structure. If the mineral has the $C2/m$ space group the number of IR and Raman bands is less than is expected for C_{2h} factor group. For C_s factor group two symmetric stretching modes would be expected. The existence of two symmetric stretching modes is registered in this work.

In case of vésigniéite, the VO_4 polyhedra exhibit considerable distorsion, that may be expressed by bond-angle distortion (variance) according to Robinson *et al.* [29], by value of 1.750 $deg.^2$. Compared to V_2O_7 polyhedra (pyrovanadate groups, consisting of interconnected VO_4 tetrahedra) of 0.746 $deg.^2$ in volborthite. Hence, the VO_4 tetrahedra in vésigniéite is less symmetrical.

In the infrared spectrum of vésigniéite in the 600 to 1200 cm^{-1} region (Fig. 6), bands at 899 cm^{-1} and at 755 and 787 cm^{-1} are attributed to the split triply degenerate ν_3 $(VO_4)^{3-}$. Botto and Deliens also assigned corresponding bands to the ν_3 $(VO_4)^{3-}$ antisymmetric stretching vibration [2]. However if there is a loss of symmetry of the vanadate anion as might be expected in a chain structure then the Raman active mode may also become infrared active and an intense band in the infrared spectrum would be expected. In the infrared spectrum an

247 additional band at 837 cm^{-1} is observed and is assigned to the ν_1 $(VO_4)^{3-}$ antisymmetric
248 stretching vibrational mode. Since the symmetry of the $(VO_4)^{3-}$ anion is reduced in the chain
249 structure of vésigniéite, it means that the infrared forbidden modes will be activated and the
250 degenerate modes will split**.** It would be expected that the ν_3 $(VO_4)^{3-}$ antisymmetric stretching
251 vibration would be of low intensity in the Raman spectrum and intense in the infrared
252 spectrum. A band at 705 cm^{-1} may be attributed to the OH bending mode. Botto and Deliens
253 observed a band of medium intensity at 765 cm^{-1} and assigned this band to the ν_3 $(VO_4)^{3-}$
254 antisymmetric stretching mode [2]. Botto and Deliens observed an infrared band at 575 cm^{-1}
255 and suggested this band was due to the OH librational mode [2]. Three bands at 1100, 1056
256 and 1019 cm^{-1} are attributed to the δ Cu-OH deformation vibrations.
257
258 The Raman spectrum of vésigniéite in the 100 to 600 cm^{-1} region is displayed in Fig.
259 7. The two Raman bands at 307 and 332 cm^{-1} are assigned to the ν_2 $(VO_4)^{3-}$ symmetric
260 bending modes. The bands at 466 and 511 cm^{-1} are ascribed to the ν_4 $(VO_4)^{3-}$ antisymmetric
261 bending mode. Botto and Deliens observed a Raman band of medium intensity at 468 cm^{-1}
262 and assigned this to the ν_2 $(VO_4)^{3-}$ symmetric bending mode [2]. However this assignment
263 may be in error as one would expect the $(VO_4)^{3-}$ symmetric bending mode to be the most
264 intense as is observed for the two bands at 307 and 332 cm^{-1}. These authors observed a very
265 low intensity band at 338 cm^{-1} and assigned this band incorrectly to the $(VO_4)^{3-}$
266 antisymmetric bending mode [2]. Two bands are observed at 355 and 371 cm^{-1}. These bands
267 may be attributed to hydrogen bonded OH units in the vésigniéite structure. An alternative
268 assignment of the 511 cm^{-1} band is to a CuO stretching mode. Botto and Deliens ascribed an
269 infrared band at 500 cm^{-1} to CuO stretching vibration [2]. Raman bands with wavenumbers
270 lower than 200 cm^{-1} located at 112, 162, 175 and 185 cm^{-1} are assigned to lattice vibrations.
271
272 The Raman spectrum of vésigniéte in the 1600 to 3600 cm^{-1} region is shown in Fig. 8.
273 Three Raman bands are observed at 1960, 2609 and 2896 cm^{-1}. The Raman band at 1960 cm^{-1}
274 may be assigned to a combination band [21]. The other two bands may be related to the ν OH
275 stretching vibrations of strongly hydrogen bonded hydroxyls [29]. In the infrared spectrum of
276 vésigniéite in the 1300 to 3800 cm^{-1} region (Fig. 9), a series of bands are observed at 1395,
277 1461, 1597, 1658, 1875, 1970, 2058, 2440 and 2580 cm^{-1}. According to Busca [21], these
278 bands are in all likelihood connected with combination bands and overtones. Another
279 complicated series of infrared bands was observed at 2754, 2860, 2922, and 2977 cm^{-1} related

also to the infrared bands observed at 3411, 3620 and 3698 cm^{-1}. These bands are attributed to the ν OH stretching modes of weakly to very strongly hydrogen bonded $(OH)^-$ units in the vésigniéte structure [30, 31]. Botto and Deliens found a broad infrared band centred at 3300 cm^{-1} and ascribed this band to the stretching mode of the OH units [2]. O-H...O hydrogen bond lengths inferred from the spectra vary approximately in the range from 2.6 to 2.9 Å (Raman) and 2.6- > 3.2 Å [30].

Raman and infrared spectra of volborthite

The Raman spectra of volborthite in the 100 to 1100 cm^{-1} and 1500 to 4000 cm^{-1} regions are shown in Figs. 10 and 11, respectively. Raman bands observed in the 749 to 891 cm^{-1} region are attributed to the ν_1 (VO_3) symmetric stretching vibrations (888 cm^{-1}), the ν_3 (VO_3) antisymmetric stretching vibrations (858, 814 and 749 cm^{-1}), and ν_3 (V-O-V) antisymmetric stretching vibrations (814 cm^{-1}) [16]. The Raman bands observed at 509 cm^{-1} are attributed to the ν_1 (V-O-V) symmetric stretching vibration. Raman bands at 476 and 442 cm^{-1} are assigned to the ν_4 (VO_3) bending vibrations and those at 347 and 308 cm^{-1} to the ν_2 (VO_3) bending vibrations. The δ (V-O-V) bending vibration is connected with the Raman bands observed at 245 cm^{-1} [16]. Bands at 180 and 118 cm^{-1} are assigned to the lattice vibrations.

Raman bands observed at 3475, 2948 and 2605 cm^{-1} are connected with the ν OH stretching vibrations of weakly hydrogen bonded hydroxyls and strongly hydrogen bonded water molecules. However, the position of the band at 2605 cm^{-1} seems too low to be assigned to hydrogen bonded water molecules. Another possible assignment is that these bands are due to organic impurities.

Infrared bands of volborthite in the 1200 to 600 cm^{-1} and 1200 to 4000 cm^{-1} are shown in Figs. 12 and 13, respectively. The band at 903 cm^{-1} are assigned to the ν_1 (VO_3) symmetric stretching vibrations, bands at 872, 844, 801, 758 to the ν_3 (VO_3) antisymmetric stretching vibrations, and shoulders at 704 and 676 cm^{-1} may be attributed to the libration modes of water molecules and/or OH bending modes. Bands at 1097, 1061 and 1023 cm^{-1} may be assigned to the δ Cu-OH bending vibrations, similarly as in the case of the infrared spectrum of vésigniéite.

Infrared bands at 1643 and 1615 cm^{-1} are assigned to the δ H_2O bending vibrations, while those at 1446, 1337 and 1990 cm^{-1} to overtones and/or combination bands. A series of bands in the 2700 to 3000 cm^{-1} region as in the case of the spectra of vésigniéite may be assigned to organic impurities, possibly on the surface of the mineral (perhaps as a result of handling). The infrared band at 3549 cm^{-1} is assigned to the ν OH stretching vibration of hydroxyl ions, and those at 3467 and 3348 cm^{-1} to the ν OH stretching vibrations of water molecules. O-H...O hydrogen bond lengths inferred from the spectra vary approximately in the range from 2.6 to 2.9 Å (Raman) and from 2.5 to 3.0 Å (infrared) [30].

CONCLUSIONS

Raman spectroscopy complemented with infrared spectroscopy has been used to study two monoclinic minerals vésigniéite (Vrančice, Czech Republic), $BaCu_3(VO_4)_2(OH)_2$, and volborthite (Ural, Russia), $Cu_3V_2O_7(OH)_2 \cdot 2H_2O$. Raman and infrared bands were assigned to the $(VO_4)^{3-}$, $(OH)^-$ and (Cu-OH) units in vésigniéite, and (VO_3), (VOV), (Cu-OH), $(OH)^-$ and H_2O in volborthite. The presence of hydrogen bonded hydroxyls in the structure of vésigniéite, and hydrogen bonded water molecules and hydroxyls in the structure of volborthite is proved. Approximate O-H...O hydrogen bond lengths were inferred from the Raman and infrared spectra. The Raman as well as the infrared spectra of both minerals are similar. Bands of their skeletal vibrations are located in the same regions, albeit crystal structures of both minerals differ.

Acknowledgements

The financial and infra-structure support of the Chemistry Discipline of the Faculty of Science and Technology of the Queensland University of Technology, is gratefully acknowledged. The Australian Research Council (ARC) is thanked for funding the instrumentation. This work was financially supported by Ministry of Culture of the Czech Republic (MK00002327201) to Jiří Sejkora and Jakub Plášil.

345 **REFERENCES**

346

347 [1] J.W. Anthony, R.A. Bideaux, K.W. Bladh, M.C. Nichols, *Handbook of Mineralogy*,
348 Vol. IV, Arsenates, Phosphates, Vanadates. Mineral Data Publishing, Tuscon,
349 Arizona, USA, 2000.
350 [2] I.L. Botto, M. Deliens, *An. Asoc. Quim. Argent.* **1988**,*76,* 341.

351 [3] C. Guillemin, Z. Johan, C. R. Hebd. *Seances Acad. Sci.,* **1976**, *D28,* 803.
352 [4] M. Zhesheng, H. Ruilin, Z. Xiaoling, *Acta Geol. Sinica,* **1991**, *4*, 145.
353 [5] M.A. Lafontaine, A. Le Bail, G. Férey, *J. Solid State Chem.* **1990**, *85*, 220.
354 [6] K. Melghit, L.S. Wen, *Ceramics Int.* **2005**, *31*, 223.
355 [7] A.A. Kashaev, I.V. Rozhdestvenskaya, I.I. Bannova, A.N. Sapozhnikov, O.D.
356 Glebova, *Zh. Strukt. Khim.* **2008**, *49*, 695 (in Russian).
357 [8] A.R. Kampf, I.M. Steele, *Can. Mineral.* **2008**, *46*, 687.
358 [9] Y. Okamoto, H. Yoshida, ZS. Hiroi, *J. Phys. Soc. Japan,* **2009**, *78*, 1.
359 [10] Z. Hiroi, H. Yoshida, Y. Okamoto, M. Takigawa, *J. Phys.: Conf. Serie,* **2009**, *145*, 1.
360 [11] R.L. Frost, K.L. Erickson, M.L. Weier, *Spectrochim. Acta* **2004**, *A60*, 2419.
361 [12] H.T. Evans, Jr., J.S. White, Jr., *Mineral. Rec.,* **1987**, *18*,333.
362 [13] S.R. Levitt, R.A. Condrate, *Am. Min.* **1970**, *55*, 1562.
363 [14] S.D. Ross, *Inorganic infrared and Raman spectra*, McGraw-Hill London, 1972.
364 [15] J.A. Gadsden, *Infrared Spectra of Minerals and Related Inorganic Compounds*,
365 Butterworth & Co., London, 1975.
366 [16] W.P. Griffith, T.D. Wickins, *J. Chem. Soc. (A), Inorg. Phys. Theor.* **1966**, 1087.
367 [17] W.P. Griffith, *Advances in Infrared and Raman Spectroscopy of Minerals*. In:
368 Spectroscopy of Inorganic-based Materials (R.J.H. Clark and R.E. Hester, Eds.), p.
369 119-186, J. Wiley & Sons Ltd., London, 1987.
370 [18] D.M. Adams, *J. Chem. Soc.* **1974**, 1505.
371 [19] S.D. Ross, *Phosphates and other Oxy-anions of Group V.* In: The Infrared spectra of
372 Minerals (V.C. Farmer, Ed.), p. 383-422. The Mineralogical Society, London, 1974.
373 [20] P.J.A. Ribeiro-Claro, A.M. Amado, J.J.C. Teixeira-Dias, *J. Comput. Chem.* 1966, 17,
374 1183.
375 [21] G. Busca, *J. Raman Spectrosc.* **2002**, *33*, 348.
376 [22] M. Schindler, F.C. Hawthorne, W.H. Baur, *Can. Mineral.* **2000**, *38*, 1443.
377 [23] M. Schindler, F.C. Hawthorne, W.H. Baur, *Chem. Mater.* **2000**, *12*, 1248.

[24] J. Sejkora, J. Čejka, V. Šrein, J. Geosc. **2007**, *52*, 199.
[25] J. Plášil, J. Sejkora, J. Čejka, P. Škácha, V. Goliáš, J. Geosc. **2009**, *54*, 15.
[26] J. Sejkora, F.C. Hawthorne, M.A. Cooper, J.D. Grice, J. Vajdak, J.L. Jambor, *Can. Mineral.* **2009**, *47*, 159.
[27] H. Siebert, *Anwendungen der Schwingungsspektroskopie in der Anorganischen Chemie,* Springer Berlin 1966.
[28] K. Nakamoto, *Infrared and Raman Spectra of Inorganic and Coordination Compounds.* J. Wiley and Sons New York 1986.
[29] K. Robinson, G.V. Gibbs, P.H. Ribbe *Science*, **1971**, *172*, 567.
[30] E. Libowitzky, *Monatshefte Chem.* **1999**, *130*, 1047.
[31] E. Libowitzky, A. Beran, *EMU Notes in Mineralogy* **2004**, *6*, 227.

Table 1

Chemical composition of vésigniéite and volborthite (wt. %)

	vésigniéite[a]			volborthite[b]		
	mean	range		mean	range	
K_2O	0.21	0.10 -	0.28	0	0 -	0
CaO	0.20	0.12 -	0.35	0.04	0.02 -	0.08
FeO	0.13	0.07 -	0.21	0.03	0.01 -	0.04
BaO	21.99	21.42 -	22.34	0.00	0.00 -	
CuO	39.84	39.55 -	40.38	49.18	48.66 -	49.37
ZnO	0.14	0.00 -	0.30	0.06	0.05 -	0.14
Al_2O_3	0.54	0.17 -	1.15	0.00	0.00 -	0.00
SiO_2	1.12	0.51 -	2.10	0.32	0.28 -	0.35
As_2O_5	1.58	1.26 -	1.74	0.00	0.00 -	0.00
P_2O_5	0.39	0.30 -	0.56	0.00	0.00 -	0.00
V_2O_5	26.63	26.33 -	27.06	37.01	36.95 -	37.35
H_2O*	2.95	2.89 -	3.08	11.08	10.98 -	11.15
Total	95.71	94.80 -	96.74	97.73	97.03 -	98.49

H_2O - content calculated on the basis of charge balance and theoretical content $2H_2O$ in volborthite.

[a] Mean and range of three point analyses.

[b] Mean and range of three point analyses.

403 **Table 2**
404 Results of the vibrational spectroscopic analyses of vesigniéite and volborthite
405

vésigniéite			volborthite		
RAMAN	IR	assignment	RAMAN	IR	assignment
3463, 2896, 2609	3699, 3624, 3415, 3213, 2922, 2919, 2860, 2754	stretching ν (OH) organic impurities (?)	3475, 2948, 2605	3549, 3467, 3348, 2961, 2955, 2924, 2844, 2854	stretching ν (OH) organic impurities (?)
1960	2580, 2440, 2058, 1970, 1872	combination band	1972, 1785 1717	1990	combination bands/overtones
1636, 1559	1658, 1597	combination bands/overtones	1617	1643, 1615	bending δ H_2O
	1461, 1395	organic impurities (?) or combination bands/overtones		1446, 1337	organic impurities (?) or combination bands/overtones
1059	1100, 1056, 1019	vibration δ (Cu-OH)		1097, 1061, 1023	vibration δ (Cu-OH)
	899	stretching $\nu_3 (VO_4)^{3-}$	888	903	stretching $\nu_1 (VO_3)$
			858	872, 844,	stretching $\nu_3 (VO_3)$
856, 821	837	stretching $\nu_1 (VO_4)^{3-}$	814		stretching ν_3 (VOV)
750	787, 755	stretching $\nu_3 (VO_4)^{3-}$	749	801, 758	stretching $\nu_3 (VO_3)$
	705	bending (OH)		704, 676	bending (OH) or H_2O libration
511, 466		bending $\nu_4 (VO_4)^{3-}$	509		stretching ν_1 (VOV)
			476, 442		bending $\nu_4 (VO_3)$
371, 355		bending $\nu_2 (VO_4)^{3-}$ (?)	347, 308		bending $\nu_2 (VO_3)$
332, 307		bending $\nu_2 (VO_4)^{3-}$			
			245		bending (VOV)
185, 175, 162, 112		lattice vibrations	180		lattice vibrations

406
407
408
409
410
411

List of Figures.

Figure 1 Crystal structure of vésigniéite in general projection. The sheets of CuO_6 octahedra (light green) are linked via hydrogen bonding (blue dotted line) of O1 (shared corner of the three octahedrons) –H1–O4 (apical oxygen of the VO_4 tetrahedra), and by Ba–O bonds (bicolored) in the interlayer.

Figure 2 Crystal structure of volborthite in general projection. The sheets of CuO_6 octahedra (light green) are linked via pyrovanadate groups (dark green) and by hydrogen bonding (blue dotted line) between layers (oxygen atom adhering to the octahedra) and water molecules in the interlayer.

Figure 3 Raman spectra of (a) vesegneite and (b) volborthite over the 4000 to 100 cm^{-1} region

Figure 4 Infrared spectra of (a) vesegneite and (b) volborthite over the 4000 to 500 cm^{-1} region

Fig. 5 Raman spectrum of vésigniéite in the 1200 to 600 cm^{-1} region

Fig. 6 Infrared spectrum of vésigniéite in the 1200 to 600 cm^{-1} region

Fig. 7 Raman spectrum of vésigniéite in the 600 to 100 cm^{-1} region

Fig. 8 Raman spectrum of vésigniéite in the 3700 to 1500 cm^{-1} region

Fig. 9 Infrared spectrum of vésigniéite in the 3800 to 1200 cm^{-1} region

Fig. 10 Raman spectrum of volborthite in the 1100 to 100 cm^{-1} region

Fig. 11 Raman spectrum of volborthite in the 3700 to 1500 cm^{-1} region

Fig. 12 Infrared spectrum of volborthite in the 1200 to 600 cm^{-1} region

445

446 **Fig. 13 Infrared spectrum of volborthite in the 3800 to 1200 cm^{-1} region**

447

448

449

List of Tables

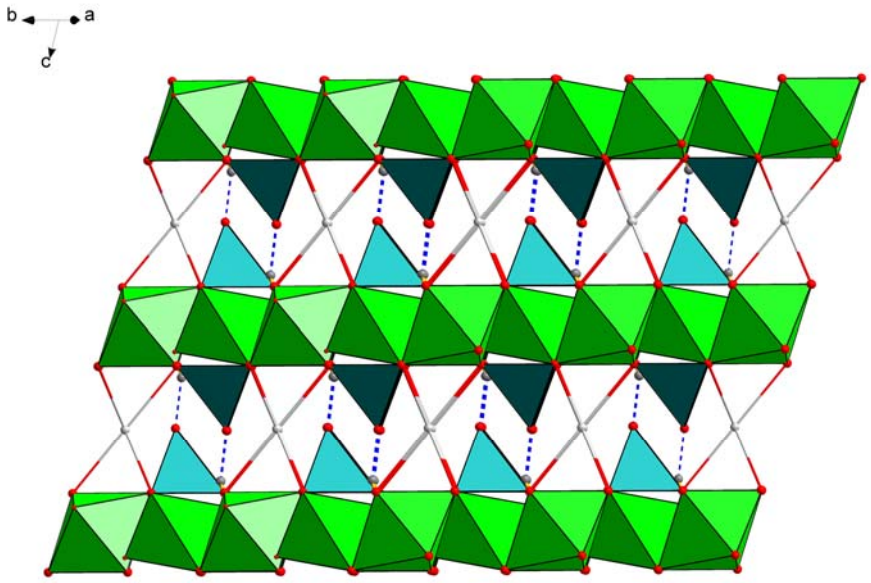

460

461 **Figure 1. Vésigniéite**

462

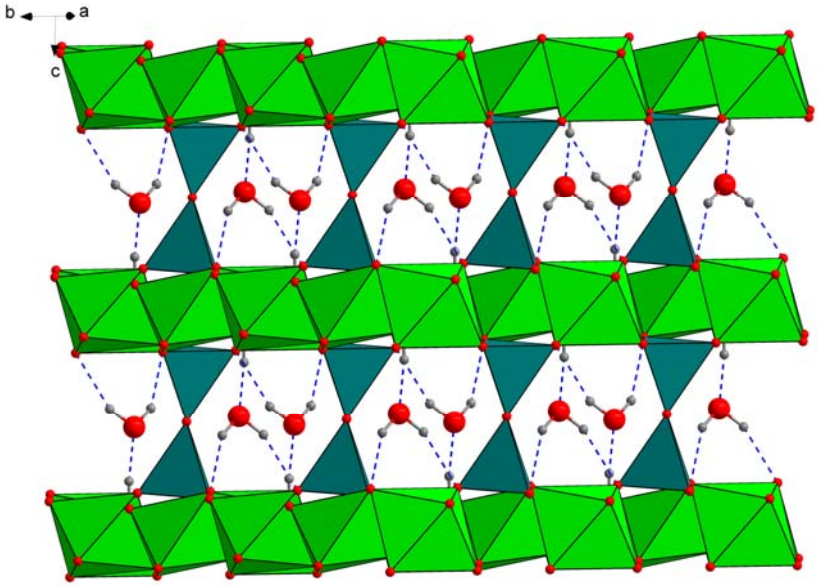

463

464 **Figure 2. Volborthite**

465

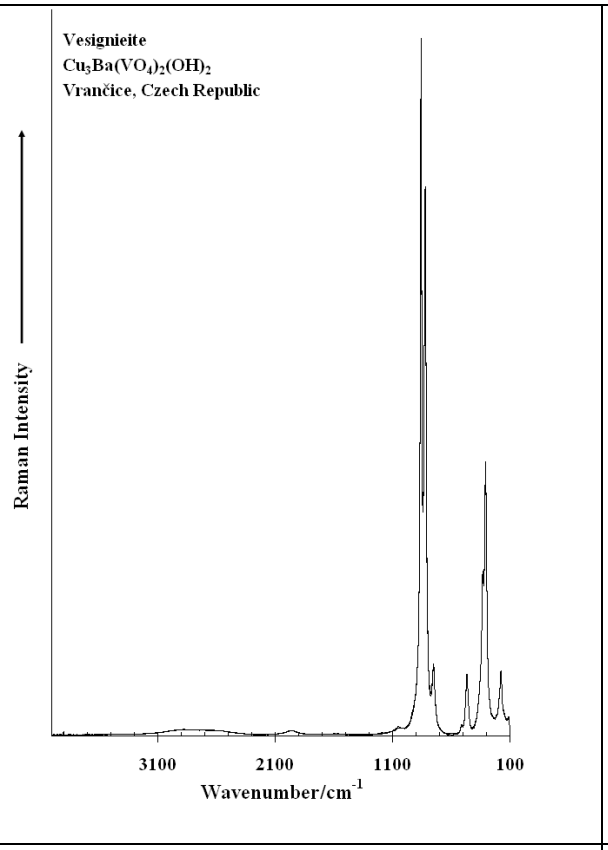

Figure 3a

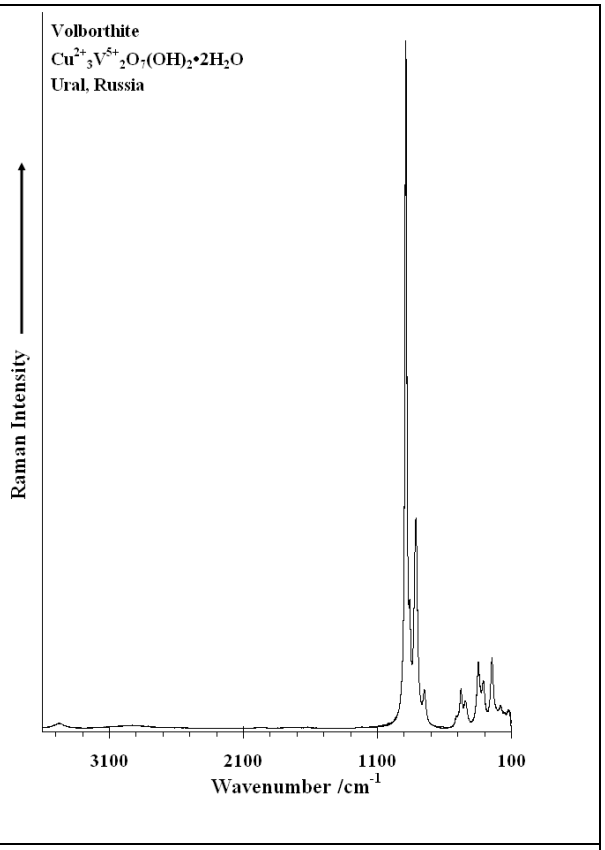

Figure 3b

466

467

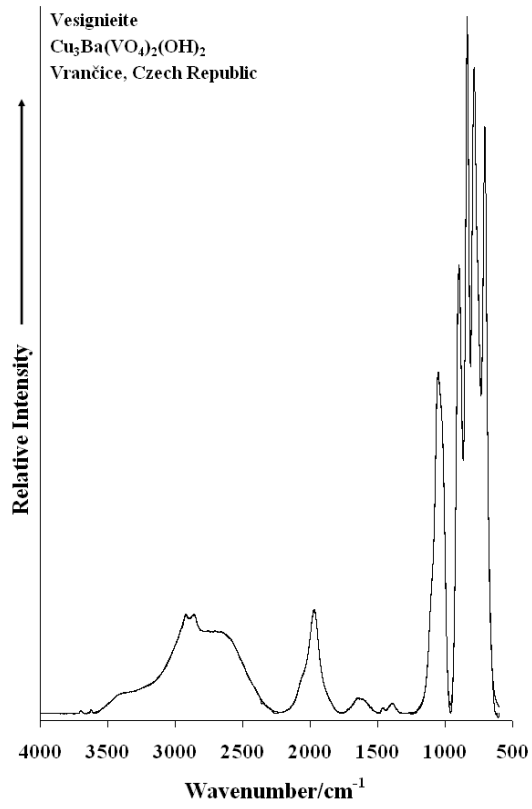

Figure 4a

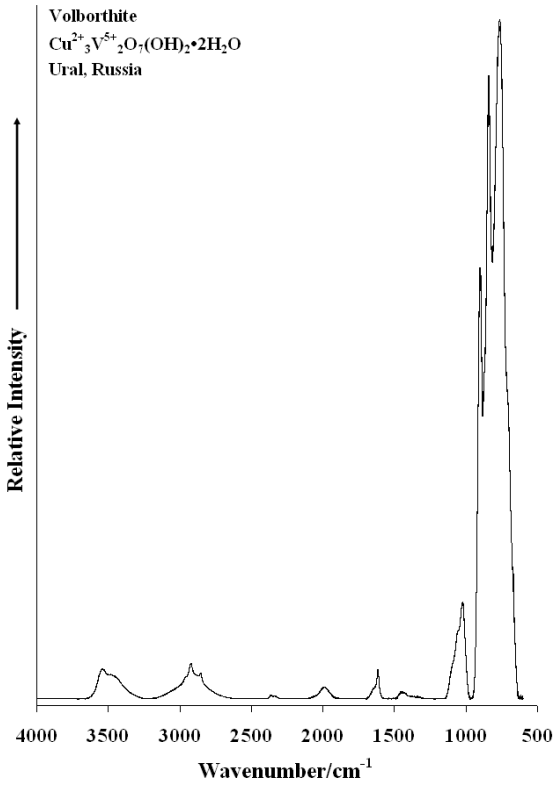

Figure 4b

468

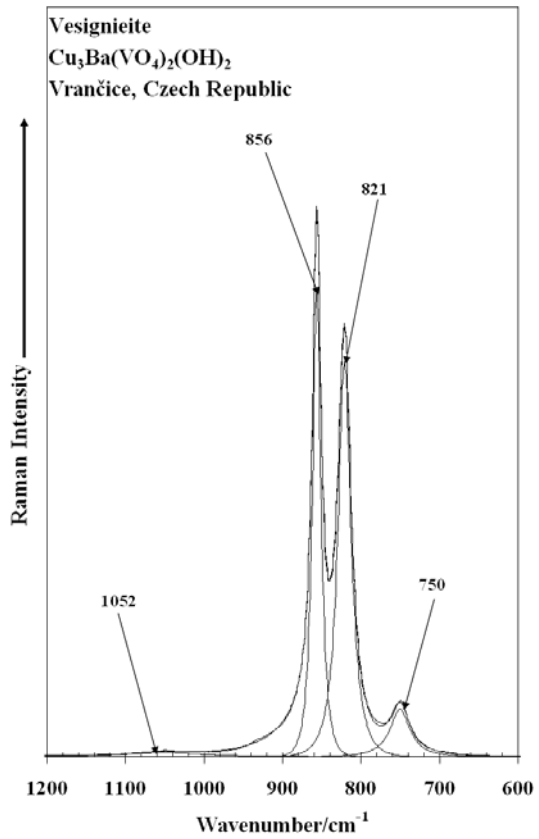

469

470

471

472 **Figure 5**

473

474

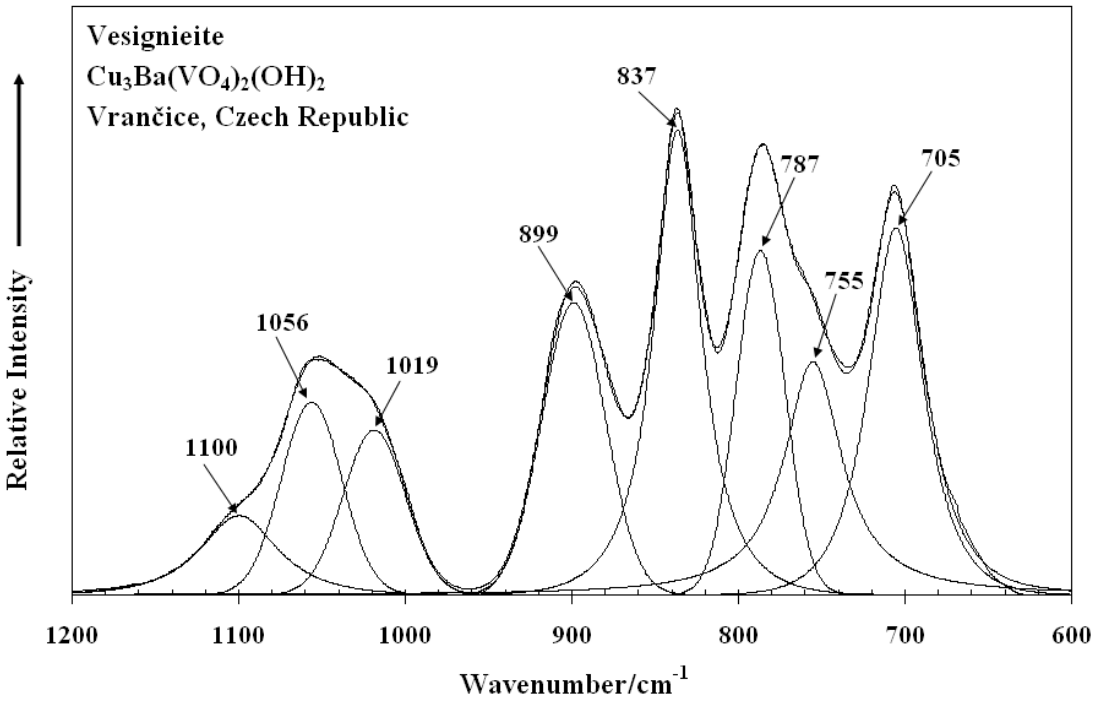

475

476

477 **Figure 6**

478

479

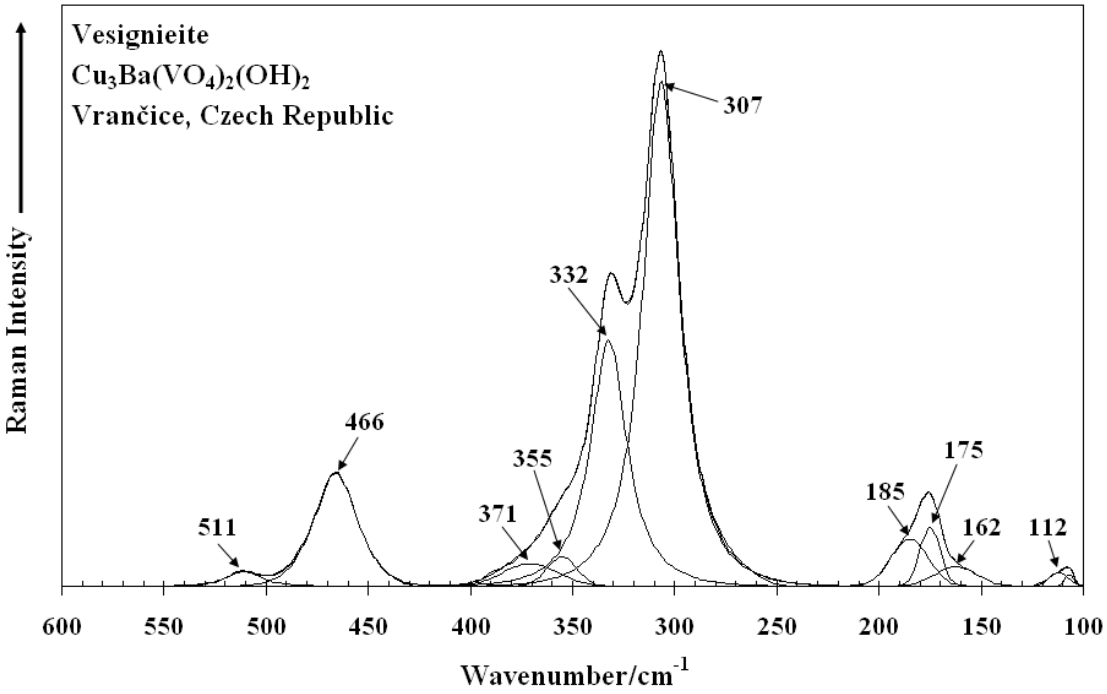

480

481

482 **Figure 7**

483

484

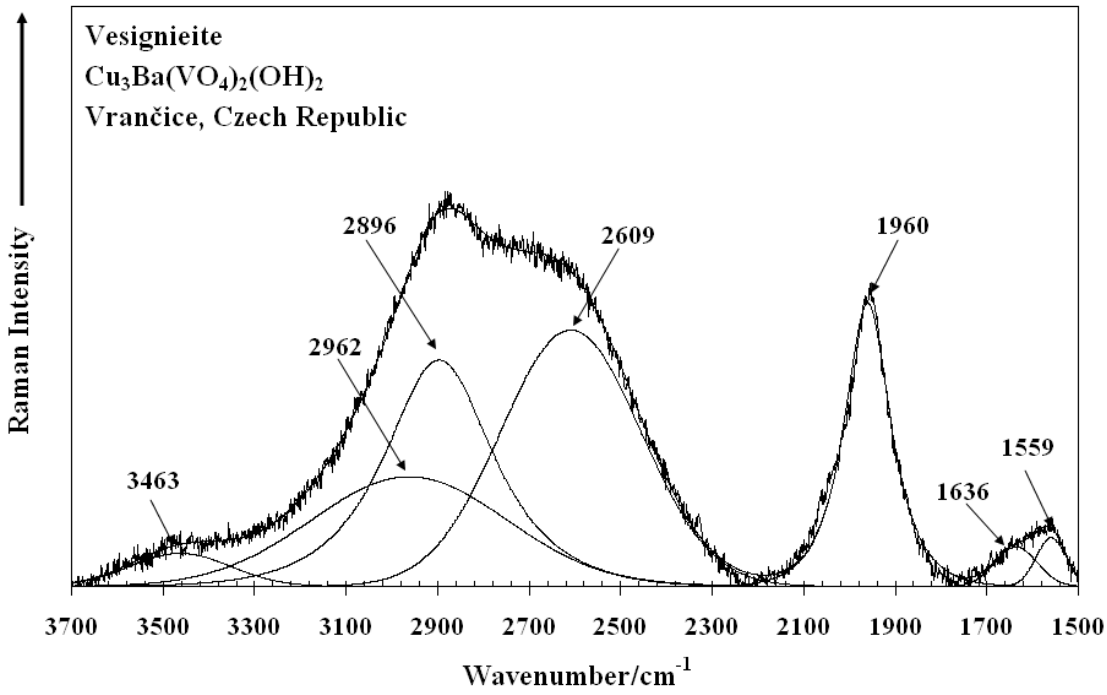

485

486

487 **Figure 8**

488

489

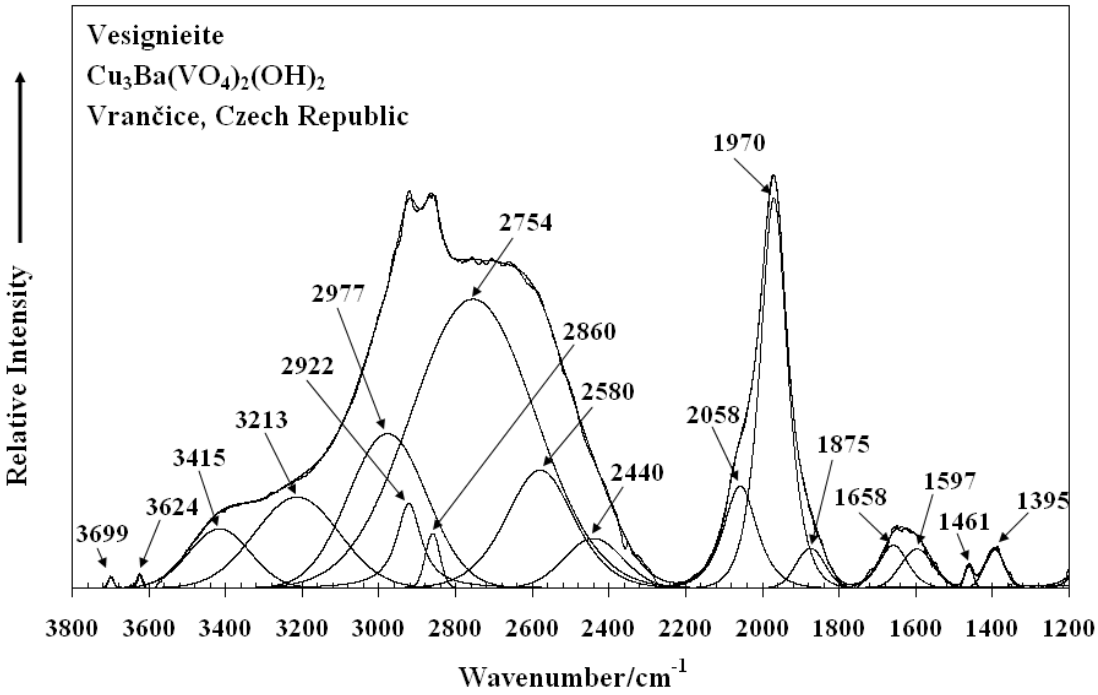

490

491

492 **Figure 9**

493

494

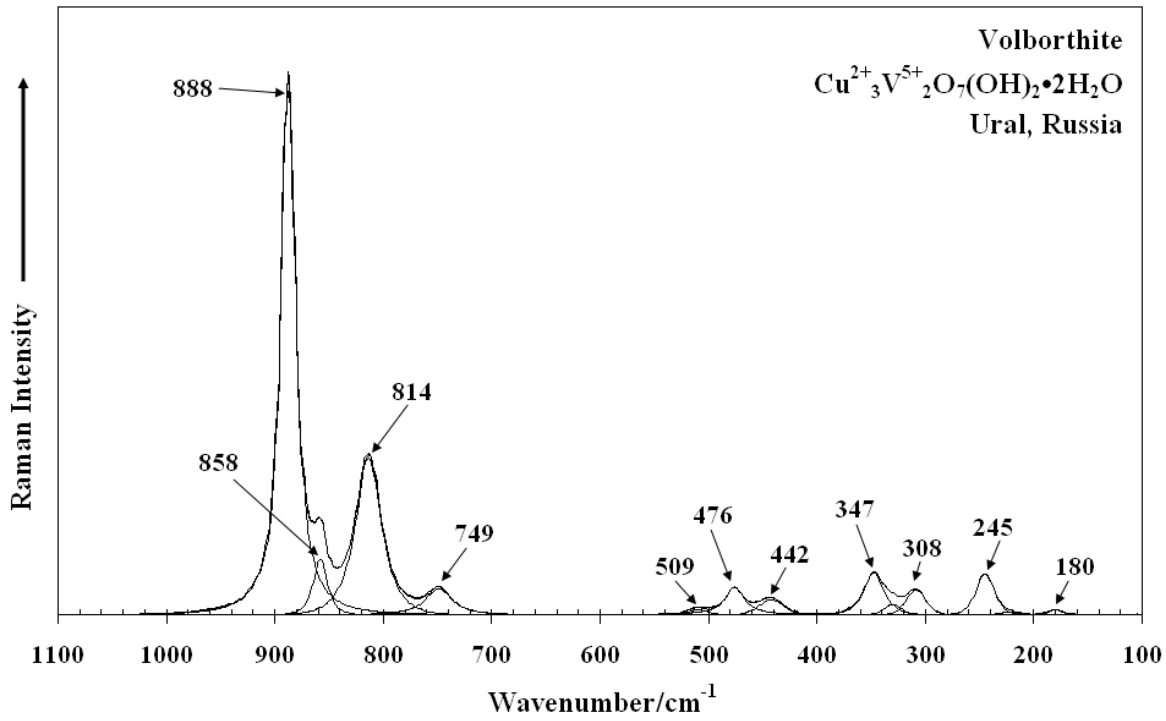
Volborthite
$Cu^{2+}_3V^{5+}_2O_7(OH)_2•2H_2O$
Ural, Russia
888
858
814
749
509
476
442
347
308
245
180
Raman Intensity
1100
1000
900
800
700
600
500
400
300
200
100
Wavenumber/cm^{-1}

Figure 10

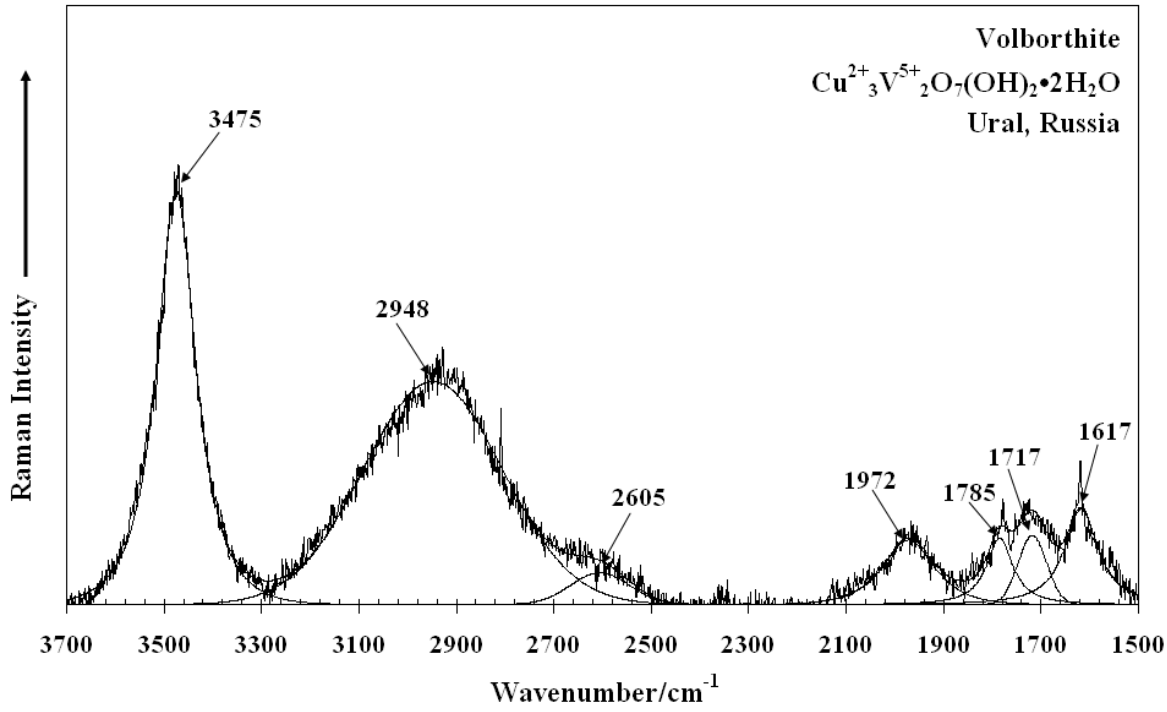
Volborthite
Cu2+3V5+2O7(OH)2•2H2O
Ural, Russia
3475
2948
2605
1972
1785
1717
1617
Raman Intensity
3700
3500
3300
3100
2900
2700
2500
2300
2100
1900
1700
1500
Wavenumber/cm-1

Figure 11

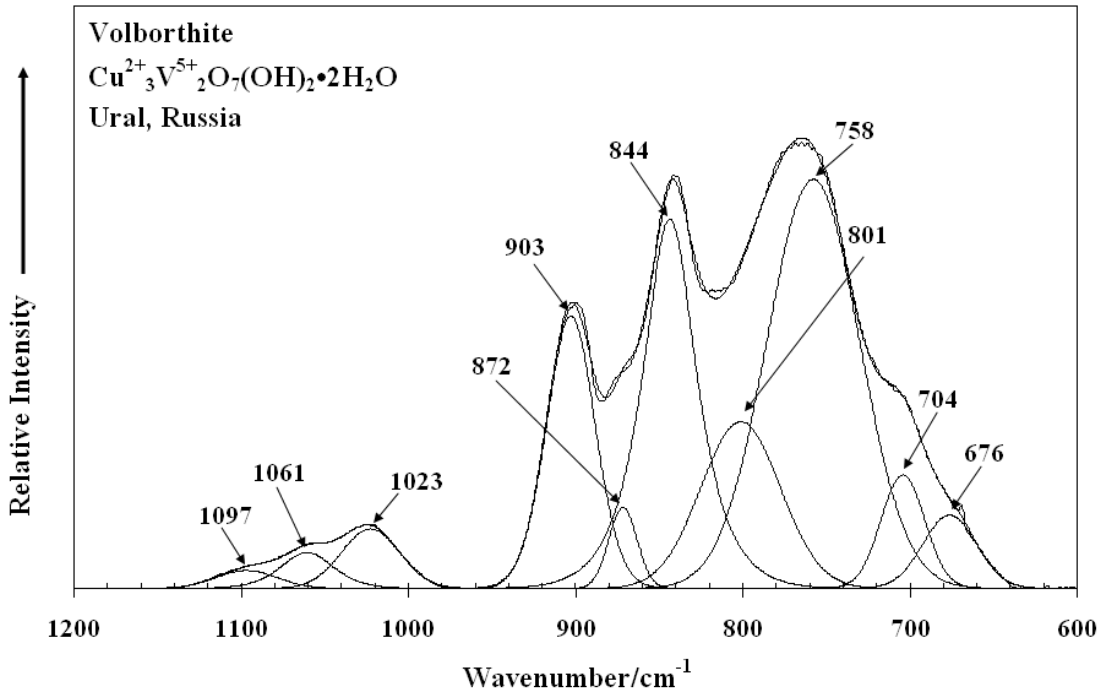

505

506

507 **Figure 12**

508

509

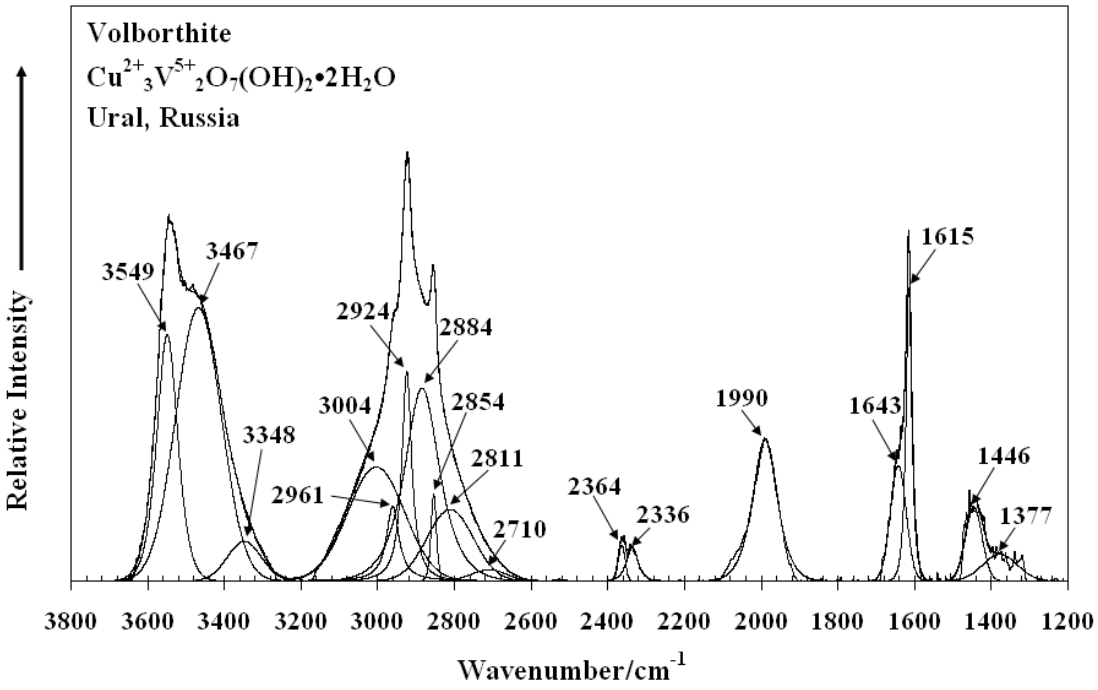

510

511

512 **Figure 13**